— 3 —

Spectroradiometry of Spatially-resolved Solar Plasma Structures

KLAUS WILHELM
Max-Planck-Institut für Aeronomie, Katlenburg-Lindau, Germany

Denn eben wo Begriffe fehlen,
da stellt ein Wort zur rechten Zeit sich ein.
J.W. v. Goethe, Faust I, Mephistopheles

The investigation of spatially-resolved solar plasma features in terms of radiometric measurements requires concepts different from those useful for full-Sun observations. After a definition of the relevant physical quantities, formulae are derived for studies of optically-thick and optically-thin plasmas observed with both spectral and spatial resolution. Simple examples of their applications to the determination of electron densities and electron temperatures as well as to studies of emission measures and elemental abundances are discussed.

3.1 Introduction

The Sun, a very close main-sequence star of spectral class G2 V, allows us to study its atmosphere in great detail, and, in particular, perform spatially-resolved observations. In these studies, not only the morphology is of importance, but also the dynamical processes in the solar plasma. Spectral information is required to disentangle this complex system. Moreover, after the atomic processes leading to the emission of radiation have been understood, the observed radiation has to be interpreted in terms of the generation processes. This calls for a quantitative investigation of the solar radiation emitted by small structures.

Since the middle of the last century, space technology has made it possible to observe the Sun in the vacuum-ultraviolet (VUV) radiation, and thus to exploit the rich information contained in the spectral emission lines and continua in this wavelength regime. The radiation is formed at temperatures corresponding to those prevailing in the solar chromosphere, transition region and corona. Early instruments had very limited or no spatial resolution at all, and, consequently, obtained Sun-as-a-star observations. Assuming specific distributions of the radiating plasmas, even then sub-resolution inferences could be drawn [cf., *Pottasch*, 1963]. However, some of the evaluation procedures established at that time have never been thoroughly adjusted so as to take into account the high spatial and spectral resolution measurements available now.

The purpose of this article is to discuss the radiometric aspects of such an adjustment in line with the standard usage of SI (The International System of Units [*BIPM*, 1998]), which explicitly lists the following quantities with special names which are relevant in this context: “power” (“radiant flux”) in units of watt (W), “irradiance” in watt per

square metre (W m^{-2}), "radiant intensity" in watt per steradian (W sr^{-1}), and "radiance" in watt per square metre steradian (W $m^{-2}sr^{-1}$). They will be supplemented by the corresponding spectrally-resolved quantities, which are usually given per nanometre (nm $^{-1}$), although many solar physicists still use per ångström ($Å^{-1}$) as the wavelength interval (1 Å = 0.1 nm).

3.2 Elementary Radiation Theory

For most solar applications, the electromagnetic VUV radiation can be thought of as emitted during transitions of electrons between different energy levels of atoms or ions. This is the case that will be considered here. Let

$$\Delta\varepsilon_{ij} \;=\; \frac{hc_0}{\lambda_{ji}} \tag{3.1}$$

be the energy difference between two levels and thus the resulting photon energy, where h is the Planck constant and c_0 is the speed of light in vacuum, then radiation with a wavelength of λ_{ji} will be emitted during the transition from the upper level j to the lower level i. For various reasons (atomic physics, thermal and non-thermal speeds of the emitters), the wavelength, λ, will exhibit a certain spread around its nominal value, λ_{ji}, generating a spectral profile of the emission line, which will be assumed here to be resolved by a spectrometer.

3.2.1 Radiation from Optically-thick Plasmas

The assumption of an optically-thick plasma is made in this section in order to establish a radiating surface. We will not discuss the radiation transfer processes inside a plasma volume. On its surface, with total area S_T, we assume in Figure 3.1 a surface element with the area dS and a normal $\boldsymbol{n}$. We then specify a solid angle $\mathbf{d}\boldsymbol{\omega}$ by

$$|\,\mathbf{d}\boldsymbol{\omega}\,| \;=\; \mathrm{d}\omega \;=\; \mathrm{d}\vartheta\,\sin\vartheta\,\mathrm{d}\psi \tag{3.2}$$

in a direction of the co-elevation angle ϑ and the azimuthal angle ψ. The spectral radiance, L_λ, is then defined by

$$\mathrm{d}Q \;=\; L_\lambda(\vartheta,\psi)\cos\vartheta\;\mathrm{d}S\,\mathrm{d}\omega\,\mathrm{d}t\,\mathrm{d}\lambda \tag{3.3}$$

where dQ is the differential radiant energy emitted from d$S\cos\vartheta$, the projected area normal to $\mathbf{d}\boldsymbol{\omega}$, at the position P_0 on the radiant surface into the solid angle $\mathbf{d}\boldsymbol{\omega}$ during the time interval $(t,\, t+\mathrm{d}t)$ and in the wavelength interval $(\lambda,\ \lambda+\mathrm{d}\lambda)$.

As indicated in Equation (3.3), L_λ is a function of λ, ϑ, and ψ (and, in general, of P_0 and t). Since the wavelength, λ, is specified, the energy, dQ, can be expressed by the number of photons, dN_λ, according to Equation (3.1) as

$$\mathrm{d}Q \;=\; \frac{hc_0}{\lambda}\,\mathrm{d}N_\lambda \tag{3.4}$$

If L_λ and all other energy-related quantities were then reckoned in photon units, one could drop the photon energy, $\Delta\varepsilon_{ij}$, from the equations. Although these photon units are

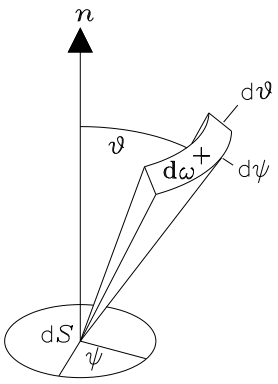

Figure 3.1: Geometrical relation of the solid angle, $\mathbf{d}\boldsymbol{\omega}$, to the surface element with an area of dS and its normal, $\boldsymbol{n}$. The co-elevation is given by the angle ϑ and the azimuth by ψ. The surface element is part of the total surface with area S_T of a plasma volume.

quite popular in the solar physics literature, we will not apply them here, because we want to follow SI definitions as much as possible. In any case, it is very important to establish for a radiometric study whether it is performed in photon or energy units.

By integrating the spectral radiance over all ψ and ϑ from 0 to $\pi/2$, we obtain the outward spectral radiant flux density

$$M_\lambda^+ \;=\; \int_{\psi=0}^{2\pi} \int_{\vartheta=0}^{\pi/2} L_\lambda(\vartheta,\,\psi)\cos\vartheta\,\sin\vartheta\;\mathrm{d}\vartheta\;\mathrm{d}\psi \tag{3.5}$$

as a function of P_0, t, and λ.

The radiant flux density is sometimes called "emittance". It corresponds to the irradiance at the source[1], i.e., a power divided by an area.

Integration of the spectral radiance over the projected surface area of the source, S', visible from the direction $(\vartheta,\,\psi)$ gives the spectral radiant intensity

$$I_\lambda(\vartheta,\,\psi) \;=\; \int_{S'} L_\lambda(\vartheta,\,\psi)\cos\vartheta\;\mathrm{d}S \;=\; \langle\, L_\lambda(\vartheta,\,\psi)\,\rangle\, S' \tag{3.6}$$

which depends on ϑ, ψ, t, and λ. The spectral intensity can be obtained by multiplying the spatially-averaged spectral radiance by the projected area, S'. Note, in particular, that the intensity is related to the total projected area of a source, and thus is helpful in characterizing a radiation field, but is not very useful in studying the structure of an extended source. For point sources ($S' = 0$), on the other hand, the *intensity* is the best choice as the quantity *radiance* cannot be defined for such an unphysical case.

[1] In the official French text of SI: "flux density" is named "flux surfacique" and "irradiance" corresponds to "éclairement énergétique" [*BIPM*, 1998].

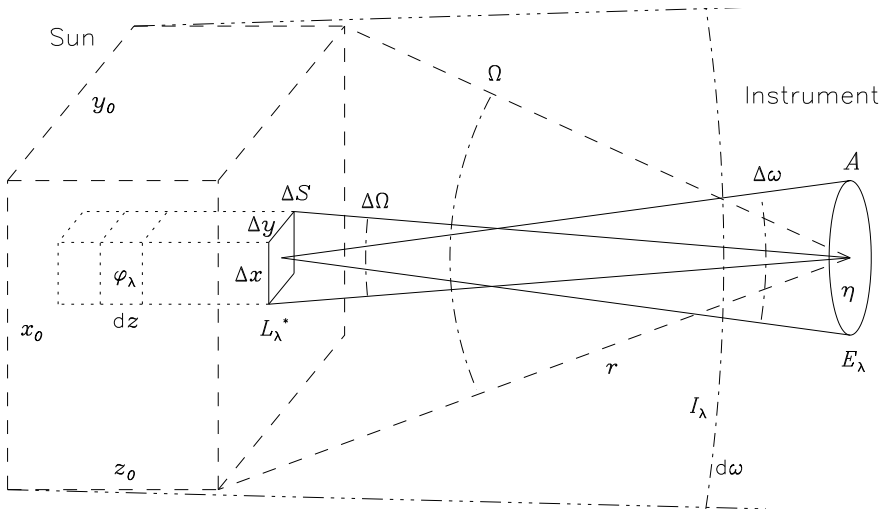

Figure 3.2: Observing geometry (schematic and not to scale) showing the principles of a radiance measurement for an optically-thick plasma (solid lines), and a generalization to the optically-thin case (dotted lines). Also sketched is an irradiance measurement (dashed lines). The solid angles are only marked by some of the extreme rays to keep the drawing simple. The spectral intensity, I_λ, is indicated in the solid angle $d\omega$ (dashed-dotted lines).

Both integration of the spectral intensity over the full sphere and integration of the spectral flux density over the total surface area yield the spectral radiant power

$$\Phi_\lambda \;=\; \int\limits_{4\pi} I_\lambda(\vartheta,\psi)\mathrm{d}\omega \;=\; \int\limits_{S_T} M_\lambda^+ \mathrm{d}S \tag{3.7}$$

Not much more can be learnt from this discussion unless specific assumptions are made that are appropriate for solar observations. As will become clear later on, very little loss of generality, as far as spatially-resolved observations are concerned, will result from assuming the following: a rectangular coordinate system ($\boldsymbol{x}$, $\boldsymbol{y}$, $\boldsymbol{z}$) with the $\boldsymbol{z}$ coordinate parallel to the viewing direction, the line of sight (LOS), of an instrument observing from a distance, r, which is much larger than all other dimensions. The radiating plasma is contained in the volume $x_0 y_0 z_0$. We now define the area, ΔS, of a surface element in accordance with the spatial resolution desired. Specifically we write

$$\Delta S \;=\; \Delta x\,\Delta y \tag{3.8}$$

with increments Δx and Δy corresponding to the linear resolution elements of the instrument. ΔS will then be perpendicular to the LOS. Since, in this case, only observations near $\vartheta \;=\; 0$ are relevant, the dependence of the radiance on the azimuth, ψ, vanishes and

$$L_\lambda^* \;=\; L_\lambda(0,\psi) \tag{3.9}$$

can be considered representing the spectral radiance within a small solid angle, $\Delta\omega$. This geometry is sketched with solid lines in Figure 3.2, where, in addition, an aperture of the

observing instrument – a telescope followed by a spectrometer – with an area, A, is shown. We then choose the size of a solid angle, $\Delta\omega$, so as to fill the aperture at a distance r from the source. Hence

$$\Delta\omega = \frac{A}{r^2} \tag{3.10}$$

and define another small solid angle centred at the position of the aperture by

$$\Delta\Omega = \frac{\Delta S}{r^2} = \frac{\Delta x\,\Delta y}{r^2} \tag{3.11}$$

This equation relates the angular resolution of the instrument to its spatial resolution at a distance r (for a technical realization see Section 3.2.2 below).

The consequences of assuming $\hat{L}_\lambda = L_\lambda(\vartheta)$ instead of Equation (3.9), i.e., $\hat{L}_\lambda$ is only dependent on ϑ, but not on ψ, are treated by *Wilhelm et al.* [1998a] and *Fontenla et al.* [1999] in the context of VUV irradiance measurements.

From Equation (3.3), applied to $\Delta\omega$ and ΔS, and with Equations (3.8 to 3.11), it follows that the radiant energy collected by the spectrometer during the sampling time Δt and in a spectral resolution element, $\Delta\lambda$, on its effective detector section is

$$\Delta Q = \overline{L^*_\lambda}\,\Delta S\,\Delta\omega\,\Delta t\,\Delta\lambda = \overline{L^*_\lambda}\,A\,\Delta\Omega\,\Delta t\,\Delta\lambda \tag{3.12}$$

where the spectral radiance is approximated by its average value in the resolution elements selected. Equation (3.12) eludicates the transition from a solid angle centred at the Sun to an instrumental geometry.

There will be a certain responsivity, η, of the detector to radiation at λ, which relates the energy, ΔQ, entering the sensitive area of the instrument to the number of output counts, ΔN_c. We define the responsivity by

$$\eta(\lambda) = \frac{\Delta N_c}{\Delta Q} \tag{3.13}$$

In realistic cases, the responsivity is a strong function of the wavelength of the radiation. In order to obtain radiometric measurements, the responsivity has to be determined by a calibration procedure, in which the radiant energy, ΔQ, must be traceable to a primary radiometric standard [cf., e.g., *Hollandt et al.*, 1996, 2002]. All the other quantities in Equations (3.12 and 3.13) require length and time measurements, which can be performed with calibrated laboratory instrumentation.

This provides the basis for a measurement of the average spectral radiance of the surface area ΔS:

$$\overline{L^*_\lambda} = \frac{\Delta N_c}{\eta\,A\,\Delta\Omega\,\Delta t\,\Delta\lambda} \tag{3.14}$$

Note that the result obtained for $\overline{L^*_\lambda}$ depends not only on the plasma conditions, but also on the choice of $\Delta\Omega$ (ΔS), Δt, and $\Delta\lambda$. Conversely, we can predict the output counts of the detector for certain observational conditions

$$\Delta N_c = \eta\,\overline{L^*_\lambda}\,A\,\Delta\Omega\,\Delta t\,\Delta\lambda = \eta\,\overline{L^*_\lambda}\,A\,\frac{\Delta S}{r^2}\,\Delta t\,\Delta\lambda \tag{3.15}$$

With given instrumental parameters η, A, $\Delta\Omega$, Δt, and $\Delta\lambda$, the number of counts is linearly related to the radiance. In particular, it is not dependent on the distance of the observing instrument from the source of the radiation. If, on the other hand, the area of the spatial resolution element, ΔS, is held constant at different distances by varying $\Delta\Omega$ according to Equation (3.11), then the number of counts is proportional to the inverse square of the distance, r, to the source for constant $\overline{L^*_\lambda}$.

3.2.2 Conceptual Optical Design

The determination of the spectral radiance according to Equation (3.14) is rather straightforward with the exception of the experimental realization of $\Delta\Omega$. In Figure 3.3 an optical design of a model instrument is drawn to demonstrate its essential features. The surface element with area ΔS is imaged through an optical system with focal length f on a detector pixel, P. The aperture stop of the design has an area of A. The field stop is represented by the pixel, P, of size $\Delta x'\,\Delta y'$. We then have from the central rays (not all are shown in the figure)

$$\Delta\Omega \;=\; \Delta\Omega' \;=\; \frac{\Delta x'\,\Delta y'}{f^2} \tag{3.16}$$

defining $\Delta\Omega$ by the pixel size and the focal length. We also find

$$\frac{\Delta x}{r} \;=\; \frac{\Delta x'}{f} \tag{3.17}$$

and

$$\frac{\Delta y}{r} \;=\; \frac{\Delta y'}{f} \tag{3.18}$$

With fixed f, $\Delta x'$, and $\Delta y'$, the linear spatial resolution elements, Δx and Δy, are proportional to the distance, r, while, of course, $\Delta\Omega$ is not dependent on r and, with reference to Equation (3.15), the output count number, ΔN_c, is constant for different r.

3.2.3 Radiation from Optically-thin Plasmas

Most of the solar upper atmosphere can be assumed to be optically thin for VUV radiation, and, consequently, these conditions have attracted quite some attention in the literature. For a discussion of principles, reference is made again to Figure 3.2, especially to the portion drawn in dotted lines and the volume element $\Delta x\,\Delta y\,\mathrm{d}z$, from which radiation is isotropically emitted (seen from a great distance). Its contribution to the spectral radiant power can be expressed as

$$\mathrm{d}\Phi_\lambda \;=\; \varphi_\lambda\,\Delta x\,\Delta y\,\mathrm{d}z \tag{3.19}$$

where φ_λ is defined as the spectral radiant power density[2], i.e., as power divided by volume. As will be outlined in the next section, φ_λ may be directly linked to the generation

[2]Compare with footnote in Section 3.2.1 and note that "power density" is "puissance volumique" [*BIPM*, 1998].

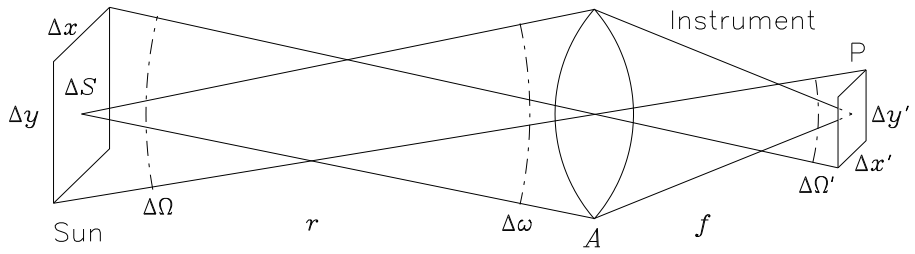

Figure 3.3: An imaging element (a lens in this model design, but a concave mirror for VUV applications) with focal length f and an aperture stop with area A projects the radiant surface element, $\Delta x\,\Delta y$, at a distance $r \gg f$ on the photon-sensitive area, $\Delta x'\,\Delta y'$, defined by the field stop, P, which usually is a detector pixel. The spectrometer portion has been omitted.

process of the radiation through the "emission measure", and thus its observational determination is one of our prime objectives.

First we calculate the contribution of the volume $\Delta x\,\Delta y\,z_0$ to the spectral irradiance, E_λ, which is incident on the surface of a sphere with radius $r \gg x_0, y_0, z_0$ centred around the total emitting volume, $x_0 y_0 z_0$. We obtain with Equation (3.11)

$$\Delta E_\lambda \;=\; \frac{\langle\varphi_\lambda\rangle\, z_0\,\Delta x\,\Delta y}{4\pi r^2} \;=\; \frac{\langle\varphi_\lambda\rangle\, z_0\,\Delta\Omega}{4\pi} \tag{3.20}$$

where

$$\langle\varphi_\lambda\rangle \;=\; \frac{1}{z_0}\int\limits_{z_0} \varphi_\lambda\,\mathrm{d}z \tag{3.21}$$

is the average spectral power density along z_0.

By considering the radiance of the surface element ΔS, we find, with the help of the definition in Equation (3.9) and Equations (3.8, 3.10, and 3.11), the irradiance at the aperture stop of the instrument as

$$\Delta E^*_\lambda \;=\; \overline{L^*_\lambda}\,\Delta x\,\Delta y\,\frac{\Delta\omega}{A} \;=\; \overline{L^*_\lambda}\Delta\Omega \tag{3.22}$$

We have used here that $\Delta\omega$ and $\Delta\Omega$ are constant to a very good approximation for positions of $\Delta x\Delta y$ along $z_0 \ll r$. We then note that ΔE_λ is uniform on the surface of the sphere under the conditions assumed. Thus

$$\Delta E_\lambda \;=\; \Delta E^*_\lambda \tag{3.23}$$

and hence, by comparing Equations (3.20 and 3.22),

$$\overline{L^*_\lambda} \;=\; \frac{\langle\varphi_\lambda\rangle\, z_0}{4\pi} \tag{3.24}$$

It should also be noted that, from summing Equation (3.22) over $x_0\, y_0$ and with Equation (3.23), it follows

$$E_\lambda \;=\; \langle L^*_\lambda \rangle\, \Omega \tag{3.25}$$

with $\Omega = x_0\, y_0 / r^2$ (Figure 5.2, dashed lines) and the average spectral radiance $\langle L^*_\lambda \rangle$ of the surface area $x_0 y_0$.

The irradiance, E_λ, can be obtained through observations either by opening up the angular acceptance cone of the instrument so as to encompass the complete radiant volume, or by covering Ω by a raster with $\Delta\Omega$, if temporal variations are slow with respect to the scan duration. The solar irradiance is often given for $r = 1$ AU if used for terrestrial applications.[3]

By combining Equations (3.14 and 3.24) the final result of this section is

$$\langle \varphi_\lambda \rangle \;=\; \frac{4\pi\, \Delta N_c}{\eta\, z_0\, A\, \Delta\Omega\, \Delta\lambda\, \Delta t} \tag{3.26}$$

which is directly applicable if z_0, the length of the LOS in the radiating plasma volume, is small compared to the structures under study. In this case we can use the approximation

$$\varphi_\lambda \;\approx\; \langle \varphi_\lambda \rangle \tag{3.27}$$

Otherwise, Equation (3.21) describes the well-known LOS problem, and $\langle \varphi_\lambda \rangle$ along z_0 is all that can be determined without additional observations or assumptions. It is, however, evident that the exact orientation of the plasma boundary near the surface is not of critical importance, because of the integration along the LOS. This justifies the assumptions of a surface element $\Delta x\, \Delta y$ perpendicular to the LOS and of L^*_λ, at least for optically-thin conditions. It might be appropriate to mention in this context that stereoscopic measurements, i.e., observations from two or more different directions, would be extremely useful in resolving such a LOS problem.

3.3 Emission Measures

The purpose of observing the Sun in the VUV is not to study radiation theory, but to extract information on the physical conditions in and the composition of the solar atmosphere. This requires an interpretation of the observed radiation in terms of processes responsible for the VUV emission. Even a summary presentation of the available literature would be far beyond the scope of this discussion. The reader is referred to the research and review articles on this topic [e.g., *Mariska*, 1980; *Raymond and Doyle*, 1981; *Mariska*, 1992; *Mason and Monsignori Fossi*, 1994; *Dwivedi*, 1994; *Dere et al.*, 1997; *Mason et al.*, 1997; *Landi et al.*, 1997]. Without further specific reference to earlier work, concepts and results obtained in the past will be re-formulated here in accordance with Section 3.2. This will first of all affect, on a formal level, the nomenclature: L_λ the spectral radiance, I_λ the spectral intensity, Φ_λ the spectral radiant power, M^+_λ the outward spectral radiant flux density, φ_λ the spectral radiant power density, and E_λ the spectral irradiance. However, it should be noted that, in most cases, the *radiance* was called *intensity* in the past, and it

[3] In *BIPM* [1998], the official unit symbol for the astronomical unit is (ua).

is not always clear whether a change is merely a formal one or not. Even the quantities *irradiance* and *radiance* have not always been unambiguously defined, which can lead to significant confusion: the irradiance is decreasing with the inverse square of the observing distance (cf., Equation (3.25)), whereas the radiance does not depend on this distance (cf., Equation (3.14)).

The quantities $\langle\varphi_\lambda\rangle$ and φ_λ in Equations (3.20, 3.24, 3.26, and 3.27) contain information on the plasma conditions. All other quantities are related to the instrumental configuration and/or the observing geometry. In order to formulate ideas, and in line with many earlier treatments, we will assume here an optically-thin solar plasma with a certain elemental abundance and ionization stages according to equilibrium conditions characterized by an electron temperature, T_e. Furthermore, only discrete states of atoms and ions excited by electron collisions from the ground state are considered, restricting the following discussion to certain classes of emission lines, but a generalization to other cases would, of course, be possible in the framework of the concepts outlined in Section 3.2. Once excited, the atoms and ions spontaneously emit photons as the main depopulation process. The probability for a transition from state j to state i is given by the Einstein coefficient, A_{ji}. This produces a radiant power density[4] in the spectral line at λ_{ji} of

$$\varphi(\lambda_{ji}) \;=\; \Delta\varepsilon_{ij}\, A_{ji}\, n_j \tag{3.28}$$

where n_j is the number density of the radiating atoms or ions in state j. The quantity $\varphi(\lambda_{ji})$ follows from φ_λ in Equation (3.19), if a wavelength range, $\delta\lambda$, can be selected in such a way that only the complete profile of the spectral line at λ_{ji} is included and if the background, b_λ, is taken out. Hence we get

$$\varphi(\lambda_{ji}) \;=\; \int\limits_{\lambda_{ji}-\delta\lambda/2}^{\lambda_{ji}+\delta\lambda/2} (\varphi_\lambda - b_\lambda)\,\mathrm{d}\lambda \tag{3.29}$$

Equations (3.26 and 3.27) provide the means of measuring φ_λ under favourable conditions or provide at least an estimate. The background has to be determined from the shape of the spectrum near the spectral line. This requires adequate spectral resolution in the measurements.

To maintain the spectral radiant power density in Equation (3.28), an excitation rate from the ground state is necessary according to

$$A_{ji}\, n_j \;=\; n_g\, n_\mathrm{e}\, C^\mathrm{e}_{gj} \tag{3.30}$$

with n_g the number density of the particles in the ground state, n_e the electron density, and C^e_{gj} the collisional excitation rate coefficient. For a Maxwellian electron velocity distribution with temperature, T_e, this coefficient is

$$C^\mathrm{e}_{gj} \;=\; \gamma\,\frac{1}{\sqrt{T_\mathrm{e}}}\,\exp\left(\frac{-\Delta\varepsilon_{gj}}{kT_\mathrm{e}}\right) \tag{3.31}$$

[4]Often called "emissivity" in the solar physics literature, whereas in Symbols, Units and Nomenclature in Physics (see Doc. U.I.P. 20, 1978) "emissivity" is defined as ratio of the emission of a surface to the corresponding black-body radiation.

where $\Delta\varepsilon_{gj}$ is the energy difference between the states g and j, and k is the Boltzmann constant. The number density, n_g, can be expressed by the ionic fraction, n_g/n_X [*Arnaud and Rothenflug*, 1985; *Arnaud and Raymond*, 1992; *Mazzotta et al.*, 1998]; the elemental abundance of X with respect to hydrogen, n_X/n_H; the number density of hydrogen relative to the electron density, n_H/n_e; and the electron density, n_e, as

$$n_g \;=\; \frac{n_g}{n_X}\,\frac{n_X}{n_H}\,\frac{n_H}{n_e}\,n_e \tag{3.32}$$

In this conceptual presentation, we will thus assume that most of the atoms or ions are in the ground state, and, in particular, n_i is small – a condition which may be violated for metastable levels. The unspecified factor γ in Equation (3.31) is of no importance here and will not be discussed any further, but will be assumed to be constant as long as a specific spectral line is being considered. From Equations (3.28 and 3.30 to 3.32), we find

$$\gamma\,\Delta\varepsilon_{ij}\,\frac{n_X}{n_H}\,\frac{n_H}{n_e}\,n_e^2\,\frac{n_g}{n_X}\,\frac{1}{\sqrt{T_e}}\exp\left(\frac{-\Delta\varepsilon_{gj}}{kT_e}\right) \;=\; \varphi(\lambda_{ji}) \tag{3.33}$$

With the definition of a contribution function

$$G(T_e) \;=\; \frac{n_g}{n_X}\,\frac{1}{\sqrt{T_e}}\exp\left(\frac{-\Delta\varepsilon_{gj}}{kT_e}\right) \tag{3.34}$$

the Equation (3.33) becomes

$$\gamma\,\Delta\varepsilon_{ij}\,\frac{n_X}{n_H}\,\frac{n_H}{n_e}\,n_e^2\,G(T_e) \;=\; \varphi(\lambda_{ji}) \tag{3.35}$$

The quantity on the right-hand side can be measured for structures with small extensions along the LOS, as we have seen in Section 3.2.3 and in Equation (3.29). In this case, some of the concepts of separating the influences of the abundance, the electron density and the temperature will be mentioned below, but they are not the main topic of this communication. For long LOS paths, z_0, we can only measure $\langle\varphi_\lambda\rangle$ and thus obtain $\langle\varphi(\lambda_{ji})\rangle$. Therefore the integral over z_0

$$\gamma\,\frac{n_H}{n_e}\,\frac{n_X}{n_H}\,\frac{\Delta\varepsilon_{ij}}{z_0}\int\limits_{z_0} n_e^2\,G(T_e)\,\mathrm{d}z \;=\; \langle\varphi(\lambda_{ji})\rangle \tag{3.36}$$

has to be considered, where the elemental abundance, which is of great importance in solar physics studies, is removed from the integral in view of the fact that, in general, the gradients of the abundance variations in the solar atmosphere are much smaller than those of the electron density and temperature. The temperature-dependent function $G(T_e)$, which is strongly peaked for most ions at the so-called "formation temperature", can also be removed from the integral, if, for instance, it can be assumed that T_e has also no gradient along z_0 (which, of course, is not generally true, but see *Feldman et al.* [1999] and *Mason et al.* [2002] for such cases). The resulting integral along z_0

$$\int\limits_{z_0} n_e^2\,\mathrm{d}z \;=\; \langle n_e^2\rangle\,z_0 \;=\; \frac{\langle\varphi(\lambda_{ji})\rangle\,z_0}{\gamma\,\Delta\varepsilon_{ij}\,G(T_e)}\,\frac{n_H}{n_X}\,\frac{n_e}{n_H} \;=\; \frac{4\pi\,L^*(\lambda_{ji})}{\gamma\,\Delta\varepsilon_{ij}\,G(T_e)}\,\frac{n_H}{n_X}\,\frac{n_e}{n_H} \tag{3.37}$$

is called "emission measure".

The radiance of the spectral line, $L^*(\lambda_{ji})$, is determined from the spectral radiance, $\overline{L^*_\lambda}$, obtained in Equation (3.14) in analogy to Equation (3.29) by integrating the background-corrected spectral radiance over the line width

$$L^*(\lambda_{ji}) = \int_{\lambda_{ji}-\delta_{\lambda/2}}^{\lambda_{ji}+\delta_{\lambda/2}} (\overline{L^*_\lambda} - B_\lambda)\,\mathrm{d}\lambda \tag{3.38}$$

Provided the spectral line can be isolated from other lines, the line radiance, $L^*(\lambda_{ji})$, does not depend on the spectral resolution of the measurement in contrast to $\overline{L^*_\lambda}$, but will still be influenced by the spatial and temporal resolution (see Section 3.2.1).

Other definitions of the emission measure, in particular the volume emission measure, are not really relevant in the context of spatially-resolved observations, but are useful in interpreting full-disk irradiance measurements [*Pottasch*, 1963; *Athay*, 1966]. The differential emission measure should only be mentioned here, but will not be discussed any further. For more information on this topic see, for example, *Mariska* [1992].

3.4 Line-ratio Measurements

3.4.1 Density-sensitive Line Ratios

For detailed treatments of the theory of density-sensitive emission see the appropriate articles cited below. Here we note that collisionally-excited states may also be depopulated by non-radiative processes, in particular, if they are metastable and if the electron density, n_e, is high. The radiant power density in Equation (3.28) is thus reduced for emission lines from such states as a function of n_e. The ratio

$$R_{12} = \frac{\varphi(\lambda_1)}{\varphi(\lambda_2)} \tag{3.39}$$

of an allowed emission line at λ_1 and a line at λ_2 emitted from a metastable level, for instance, is consequently changing with n_e, and can be calculated from atomic physics principles. If the ratio can be measured in a plasma of the solar atmosphere, the electron density can then be estimated. From Equations (3.24 or 3.37), we may conclude that this can be accomplished by measuring the ratio of the line radiances

$$R_{12} = \frac{L^*(\lambda_1)}{L^*(\lambda_2)} \tag{3.40}$$

This method is especially useful if both spectral lines are emitted by atomic particles of the same species and ionization stage, because abundance and ionization variations will then have no effect. It has been used extensively in the literature [cf., *Gabriel and Jordan*, 1969; *Feldman et al.*, 1978; *Laming et al.*, 1997; *Doschek et al.*, 1997; *Wilhelm et al.*, 1998b].

Under favourable conditions the electron density so determined can be compared with the mean electron density obtained from the emission measure analysis in Equation (3.37).

Any discrepancy points to the fact that the so-called "filling factor" is not unity [*Feldman et al.*, 1979; *Dere et al.*, 1987], because the line-ratio method provides an estimate of the electron density at the source of the radiation, whereas the emission measure depends on the distribution of the electrons within the unresolved emitting volume.

3.4.2 Temperature-sensitive Line Ratios

If two excited states, j_1 and j_2, from which emission lines originate, have very different energy levels, their relative collisional excitation becomes a function of the electron temperature, T_e. As in Section 3.4.1, a ratio R_{12} can be obtained from atomic physics calculations. The measured ratio of the line radiances in Equation (3.40) then provides a handle on the determination of the electron temperature. For examples see *Heroux et al.* [1972], *Doschek and Feldman* [1987], and *David et al.* [1998].

3.5 Abundance Measurements

If, in Equation (3.35), we consider two emission lines at λ_1 and λ_2 from different species, but with very similar contribution functions, emitted from the same location in the solar atmosphere, and thus at the same electron density, then the ratio of the radiant power densities, $\varphi(\lambda_1)$ and $\varphi(\lambda_2)$, or, from Equation (3.37), the ratio of the corresponding line radiances (adjusted for any variations of $\Delta\varepsilon_{ij}$ and γ), can be used to obtain the elemental abundance ratio. The spectral lines of Mg VI and Ne VI may serve as examples, as well as those of Mg VII and Ne VII, which have been treated by *Young and Mason* [1997], *Laming et al.* [1999], and *Dwivedi et al.* [1999] as typical species with low and high first-ionization potentials.

3.6 Concluding Remarks

The spectral radiance and the radiance of emission lines in the VUV wavelength range are described as the basic physical quantities for characterizing spatially-resolved radiant sources, such as the Sun or features in the solar atmosphere. The relationship to other radiometric quantities, in particular to radiant power (flux), emittance, power density, irradiance, and intensity is discussed in detail, as well as the observational determination of these quantities in optically-thick or optically-thin plasma regimes. Some methods of interpreting the observations in terms of the plasma conditions in the source regions are mentioned with reference to a selection of the relevant literature.

Acknowledgements

I thank A. Pauluhn, C.D. Pike, and B. Inhester for many valuable comments and suggestions.

Bibliography

Arnaud, M., and Rothenflug, R., An updated evaluation of recombination and ionization rates, *Astron. Astrophys. Suppl. Ser.* **60**, 425–457, 1985.

Arnaud, M., and Raymond, J., Iron ionization and recombination rates and ionization equilibrium, *Astrophys. J.* **398**, 394–406, 1992.

Athay, R.G., Radiative energy loss from the solar chromosphere and corona, *Astrophys. J.* **146**, 223–240, 1966.

BIPM (Bureau International des Poids et Mesures), Le Système International d'Unités (SI) and The International System of Units, 7th ed., Sèvres, France, 1998.

David, C., Gabriel, A.H., Bely-Dubau, F., Fludra, A., Lemaire, P., and Wilhelm, K., Measurement of the electron temperature gradient in a solar coronal hole, *Astron. Astrophys.* **336**, L90–L94, 1998.

Dere, K.P., Bartoe, J.-D.F., Brueckner, G.E., Cook, J.W., and Socker, D.G., Discrete subresolution structures in the solar transition zone, *Sol. Phys.* **114**, 223–237, 1987.

Dere, K.P., Landi. E., Mason, H.E., Monsignori Fossi, B.C., and Young, P.R., CHIANTI – an atomic database for emission lines. I. Wavelengths greater than 50 Å, *Astron. Astrophys. Suppl. Ser.* **125**, 149–173, 1997.

Doschek, G.A., and Feldman, U., Ultraviolet Al III emission lines and the physics of the solar transition region, *Astrophys. J.* **315**, L67–L70, 1987.

Doschek, G.A., Warren, H.P., Laming, J.M., Mariska, J.T., Wilhelm, K., Lemaire, P., Schühle, U., and Moran, T.G., Electron densities in the solar polar coronal holes from density-sensitive line ratios of Si VIII and S X, *Astrophys. J.* **482**, L109–L112, 1997.

Dwivedi, B.N., EUV spectroscopy as a plasma diagnostic, *Space Sci. Rev.* **65**, 289–316, 1994.

Dwivedi, B.N., Curdt, W., and Wilhelm, K., Analysis of extreme-ultraviolet off-limb spectra obtained with SUMER/SOHO: Ne VI/Mg VI emission lines, *Astrophys. J.* **517**, 516–525, 1999.

Feldman, U., Doschek, G.A., Mariska, J.T., Bhatia, A.K., and Mason, H.E., Electron densities in the corona from density-sensitive line ratios in the N I isoelectronic sequence, *Astrophys. J.* **226**, 674–678, 1978.

Feldman, U., Doschek, G.A., and Mariska, J.T., On the structure of the solar transition zone and lower corona, *Astrophys. J.* **229**, 369–374, 1979.

Feldman, U., Doschek, G.A., Schühle, U., and Wilhelm, K., Properties of quiet-Sun coronal plasmas at distances of $1.04 \leq R_{\odot} \leq 1.50$ along the solar equatorial plane, *Astrophys. J.* **518**, 500–507, 1999.

Fontenla, J., White, O.R., Fox, P.A., Avrett, E.H., and Kurucz, R.L., Calculation of solar irradiances. I. Synthesis of the solar spectrum, *Astrophys. J.* **518**, 480–499, 1999.

Gabriel, A.H., and Jordan, C., Interpretation of solar helium-like ion line intensities, *Mon. Not. R. Astr. Soc.* **145**, 241–248, 1969.

Heroux, L., Cohen, M., and Malinovsky, M., The interpretation of XUV rocket measurements of intensity ratios of solar spectral lines of the lithiumlike ions O VI, Ne VIII, and Mg X, *Sol. Phys.* **23**, 369–393, 1972.

Hollandt, J., Schühle, U., Paustian, W., Curdt, W., Kühne, M., Wende, B., and Wilhelm, K., Radiometric calibration of the telescope and ultraviolet spectrometer SUMER on SOHO, *Appl. Opt.* **35**, 5125–5133, 1996.

Hollandt, J., Kühne, M., Huber, M.C.E., and Wende, B., Source standards for the radiometric calibration of astronomical telescopes in the VUV spectral range traceable to the primary standard BESSY, this volume, 2002.

Laming, J.M., Feldman, U., Schühle, U., Lemaire, P., Curdt, W., and Wilhelm, K., Electron density diagnostics for the solar upper atmosphere from spectra obtained by

SUMER/SOHO, *Astrophys. J.* **485**, 911–919, 1997.

Laming, J.M., Feldman, U., Drake, J.J., and Lemaire, P., The off-limb behavior of the first ionization potential effect in $T > 5 \times 10^5$ K solar plasmas, *Astrophys. J.* **518**, 926–936, 1999.

Landi, E., Landini, M., Pike, C.D., and Mason, H.E., SOHO CDS-NIS in-flight intensity calibration using a plasma diagnostic method, *Sol. Phys.* **175**, 553–570, 1997.

Mariska, J.T., Relative chemical abundances in different solar regions, *Astrophys. J.* **235**, 268–273, 1980.

Mariska, J.T., The solar transition region, *Cambridge Astrophysics Series*, **23**, University Press, Cambridge, 1992.

Mason, H.E., and Monsignori Fossi, B.C., Spectroscopic diagnostics in the VUV for solar and stellar plasmas, *Astron. Astrophys. Rev.* **6**, 123–179, 1994.

Mason, H.E., Young, P.R., Pike, C.D., Harrison, R.A., Fludra, A., Bromage, B.J.I., and Del Zanna, G., Application of spectroscopic diagnostics to early observations with the SOHO Coronal Diagnostic Spectrometer, *Sol. Phys.* **170**, 143–161, 1997.

Mason, H.E., Del Zanna, G., Dere, K.P., Landi, E., Landini, M., and Young, P.R., Evaluating CHIANTI and atomic data: Cases of SOHO (CDS, SUMER, EIT) and SERTS, this volume, 2002.

Mazzotta, P., Mazzitelli, G., Colafrancesco, S., and Vittorio, N., Ionization balance for optically thin plasmas: Rate coefficients for all atoms and ions of the elements H to Ni, *Astron. Astrophys. Suppl. Ser.* **133**, 403–409, 1998.

Pottasch, S.R., The lower solar corona: Interpretation of the ultraviolet spectrum, *Astrophys. J.* **137**, 945–966, 1963.

Raymond, J.C., and Doyle, J.G., Emissivities of strong ultraviolet lines, *Astrophys. J.* **245**, 1141–1144, 1981.

Young, P.R., and Mason, H.E., The Mg/Ne abundance ratio in a recently emerged flux region observed by CDS, *Sol. Phys.* **175**, 523–539, 1997.

Wilhelm, K., Lemaire, P., Dammasch, I.E., Hollandt, J., Schühle, U., Curdt, W., Kucera, T., Hassler, D.M., and Huber, M.C.E., Solar irradiances and radiances of UV and EUV lines during the minimum of the sunspot activity in 1996, *Astron. Astrophys.* **334**, 685–702, 1998a.

Wilhelm, K., Marsch, E., Dwivedi, B.N., Hassler, D.M., Lemaire, P., Gabriel, A.H., and Huber, M.C.E., The solar corona above polar coronal holes as seen by SUMER on SOHO, *Astrophys. J.* **500**, 1023–1038, 1998b.